Environmental Pollution 242 (2018) 986–993

Contents lists available at ScienceDirect

Environmental Pollution

journal homepage: www.elsevier.com/locate/envpol

Thiosulphate-induced phytoextraction of mercury in *Brassica juncea*: Spectroscopic investigations to define a mechanism for Hg uptake☆

Jianxu Wang [a, b], Christopher W.N. Anderson [c], Ying Xing [d], Yuhong Fan [a], Jicheng Xia [a, e], Sabry M. Shaheen [f, b], Jörg Rinklebe [b, g], Xinbin Feng [a, *]

[a] State Key Laboratory of Environmental Geochemistry, Institute of Geochemistry, Chinese Academy of Sciences, 550082, Guiyang, PR China
[b] University of Wuppertal, School of Architecture and Civil Engineering, Institute of Foundation Engineering, Water- and Waste-Management, Laboratory of Soil- and Groundwater-Management, Pauluskirchstraße 7, 42285, Wuppertal, Germany
[c] Environmental Sciences, School of Agriculture and Environment, Massey University, 4442, Palmerston North, New Zealand
[d] School of Chemistry and Materials Science, Guizhou Normal University, 550002, Guiyang, China
[e] University of Chinese Academy of Sciences, 100049, Beijing, China
[f] University of Kafrelsheikh, Faculty of Agriculture, Department of Soil and Water Sciences, 33516, Kafr El-Sheikh, Egypt
[g] University of Sejong, Department of Environment, Energy and Geoinformatics, 98 Gunja-Dong, Guangjin-Gu, Seoul, Republic of Korea

ARTICLE INFO

Article history:
Received 28 April 2018
Received in revised form
12 July 2018
Accepted 15 July 2018
Available online 17 July 2018

Keywords:
Mercury
Phytoremediation
Mobilizing agents
Spectroscopic techniques
Plasma membrane permeability

ABSTRACT

Thiosulphate is extensively used to enhance mercury (Hg) phytoextraction due to its efficient in prompting plant Hg uptake. However, the mechanism by which thiosulphate promotes Hg uptake is poorly understood. We determined the concentrations of Hg and potassium (K), and their spatial distribution, in the tissues of *Brassica juncea* grown in Hg-contaminated soils treated by thiosulphate and compared this to a non-treated soil (control). The spatial distribution of Hg and K was characterized using micro-X ray fluorescence spectroscopy. The subcellular localization and speciation of Hg in the root of plant treated by thiosulphate were elucidated using Transmission electron microscope coupled energy-dispersive X-ray (TEM-EDX) spectroscopy. Thiosulphate increased significantly the Hg concentration in the roots (mainly in the epidermis and xylem) and shoots (mainly in the vascular bundles), while Hg was accumulated in the root (mainly in the epidermis) of the control plant. Thiosulphate promoted the movement of Hg from the epidermis to the xylem of roots, with subsequent loading into the stem via vascular bundles. Thiosulphate decreased the K concentration in plant tissues, relative to the control plant, and we propose this is due to leakage of electrolyte from roots via increased plasma membrane permeability as a consequence of physiological damage caused by the added thiosulphate. Mercury was distributed mainly at the extracellular space in the roots and was shown by TEM-EDX to be predominately amorphous nano-clusters of HgS. We conclude that thiosulphate-promoted Hg accumulation in the plant may happen through increased plasma membrane permeability, a changed pathway of Hg movement within plants, and extracellular co-transportation of Hg-S complexes in the roots. Our results may underpin the ongoing development of phytomanagement as an environmental strategy for Hg contaminated soils around the world.

1. Introduction

Mercury (Hg) is a extremely toxic and mobile metal that represents a severe hazard to human health (Antoniadis et al., 2017a; Beckers and Rinklebe, 2017). Mercury and its compounds remain used in Polyvinyl chloride (PVC), fluorescent lamp, mercuric thermometers, and monometer production (Zhang et al., 2015a) and poor management of Hg wastes has resulted in many incidences of extensive environmental contamination with Hg. Many countries have therefore adopted the Minamata Convention as a mechanism to mitigate human exposure to Hg. China is regarded as the largest producer and consumer of Hg in the world (Feng and Qiu, 2008). In a recent nationwide survey of soil quality the Chinese government found that nearly 1.6% of all soil samples were contaminated with

☆ This paper has been recommended for acceptance by Prof. W. Wen-Xiong.

* Corresponding author.
E-mail addresses: wangjianxu@vip.gyig.ac.cn (J. Wang), C.W.N.Anderson@massey.ac.nz (C.W.N. Anderson), smshaheen@agr.kfs.edu.eg (S.M. Shaheen), rinklebe@uni-wuppertal.de (J. Rinklebe), fengxinbin@vip.skleg.cn (X. Feng).

https://doi.org/10.1016/j.envpol.2018.07.065
0269-7491/

Hg (Zhao et al., 2015).

The transfer of Hg in soil-plant chain poses a health risk to human health. Inorganic Hg can be converted to methylmercury (MeHg) by microorganisms under anaerobic conditions, such as in rice paddies and consequently rice accumulates elevated MeHg concentrations in the edible rice grains (Zhang et al., 2010). As rice is the main staple food in China and beyond, the current status of soil Hg contamination causes social anxiety because people are increasingly aware that they might be exposed to MeHg by consuming MeHg-contaminated rice (Zhang et al., 2010). China, therefore, faces great challenges in managing the risk of Hg in soils. Increasing public awareness of this issue has driven widespread interest in the development of appropriate technologies to remediate Hg-contaminated soils.

Phytoextraction is recommended as one option for reducing toxic element content as the technology is perceived to be eco-friendly, effective, and affordable (Shaheen and Rinklebe, 2015a; Antoniadis et al., 2017b). Few phytoextraction projects have targeted the remediation of Hg-contaminated soils because no plant species have been identified to hyper-accumulate this element. Mercury phytoextraction therefore relies on mobilizing agents to promote the rate of uptake of Hg in plants (Moreno et al., 2005; Lomonte et al., 2011; Wang et al., 2012a). Many chemical ligands, including HCl (Rodríguez et al., 2016), Ethylenediaminetetraacetic acid (EDTA) (Rodríguez et al., 2016), nitrilotriacetic acid (NTA) (Beata and Katarzyna, 2012), thiosulphate (Wang et al., 2011), have been used for Hg phytoextraction (Appendix A in Table S1). Amongst these, thiosulphate appears to be the most effective for Hg phytoextraction because it induces the transformation of Hg from less bioavailable to bioavailable fractions, which can be preferentially accumulated by plants and this can lead to an overall reduction of the level of labile Hg in soils (Pedron et al., 2013; Wang et al., 2017). Moreover, use of thiosulphate leads to low risk of Hg leaching down the soil profile under field condition (Wang et al., 2014). Of the many plant species that have been used for Hg phytoextraction, *Brassica juncea* has been found significant application to Hg remediation. *Brassica juncea* is a high biomass and bioenergy crop and has the potential for multiple element accumulations, and is thought to be tolerant to Hg-induced stress due to the existence of an metabolic defense and adaption system (Shiyab et al., 2009). Thiosulphate-assisted phytoextraction using *Brassica juncea* can therefore be considered as a viable technology to reduce the risk of bioavailable Hg in soils around industrial sites and Hg mining areas (Pedron et al., 2013; Wang et al., 2014).

The significant increase in Hg concentration in plants treated with thiosulphate suggests a physiological mechanism associated with Hg transportation and sequestration within plants. However, there is limited understanding of the mechanism by which Hg can cross the root plasma membrane and be subsequently loaded into aboveground tissues after thiosulphate treatment. One possible mechanism is the transfer of soluble ions into roots as a consequence of cell membrane damage (Luo et al., 2008). Potassium (K) leakage from plant tissues is an indicator of cell membrane damage (Wei et al., 2008; Zheng et al., 2008), and following this theory, comparison of the K concentration between control and thiosulphate treated plants could qualify the extent of damage to the cell plasma membrane.

In the current work we aimed to address the lack of knowledge on the possible mechanisms of thiosulphate-induced Hg accumulation and translocation by *Brassica juncea*. The specific objectives of our study were to i) verify the ability of *B.juncea* to accumulate Hg from a contaminated soil treated with thiosulphate; ii) investigate the effect of thiosulphate on Hg accumulation in plants using the plant's K concentration as an indicator of the permeability of the cell plasma membrane; iii) visualize the spatial distribution of Hg and K in the roots and stems of *B. juncea* in thiosulphate-treated and untreated soils using μ-XRF spectroscopy; and iv) to explore the speciation and subcellular distribution of Hg in the roots of thiosulphate treated plants using TEM-EDX spectrocopy. The development of an appropriate knowledge to the topic is a critical step towards a better understanding of the mechanism of thiosulphate induced Hg accumulation in plants. Mechanistic knowledge of this process should lead to improvements in the efficacy of thiosulphate-induced Hg phytoextraction by bioenergy crops such as *B.juncea*.

2. Materials and methods

2.1. Experimental design

2.1.1. Pot experiment

An uncontaminated soil was collected from Huaxi Village, a suburb of Guiyang city, China, with a background value of 0.3 ± 0.1 mg total Hg kg^{-1} soil ($n = 3$) then air-dried and passed through a 4-mm sieve before use. The soil is weakly alkaline (pH = 7.2) with organic matter content of about 5.7% (Zhou et al., 2015). Plastic pots (0.35L) were filled with air-dried soil, and spiked with soluble $HgCl_2$ at three levels: 0.3 mg Hg kg^{-1} soil (Hg 0.3; background level); 2.7 mg Hg kg^{-1}soil (Hg 2.7); and 20 mg Hg kg^{-1}soil (Hg 20). Each soil Hg level had two treatments (untreated and thiosulphate-treated) with three replicates per treatment. The three soil Hg concentrations used in this experiment were the common levels of Hg (from 0.1 to more than 10 mg kg^{-1}) in anthropogenically impacted lands in China (Wang et al., 2016). To prepare the Hg2.7 and Hg20 mg kg^{-1} Hg-contaminated soil, a calculated amount of 200 mg L^{-1} $HgCl_2$ solution was slowly added to soil to increase the soil Hg concentration, while avoiding leachate release from the pots. Spiked soil was incubated for 10 days to allow Hg^{2+} to reach chemical equilibrium (Shaheen and Rinklebe, 2015b). Then five seeds were sown directly into each pot. One week after germination, plants were thinned to leave one seedling per pot. The pots were arranged in a randomized block design with an average humidity of 50–70% and a diurnal temperature of 23–28 °C. Purified water was provided to the pots daily to maintain plant growth. Plants were maintained for 42 days, and on day 37, 8 mL of 1M $NH_4(S_2O_3)_2$ solution was added to pots to achieve a concentration of 8 g of $NH_4(S_2O_3)_2$ per kg of soil (Wang et al., 2014). To avoid any affect of fertilizer on the concentration of K in the soils, no fertilizer was added to the pots during plant growth. Five days after adding thiosulphate, plants were harvested and divided into shoots and roots. Plant tissues were washed thoroughly with purified water, then with deionized water and subsequently freeze-dried. The wet and dry weights of plant tissue were recorded.

2.1.2. Hydroponic experiment

Approximately 14-day old *B. juncea* seedlings were transplanted to 1.5L-plastic containers containing modified Hoagland solution (pH 5.5) in which $MgSO_4$, $ZnSO_4$, and $CuSO_4$ were replaced with $MgCl_2$, $ZnCl_2$ and $CuCl_2$ respectively to avoid the potential impact of sulfate on the interactions between thiosulphate and Hg^{2+}. After 5 days of incubation, about 0.5 mM $HgCl_2$ and $S_2O_3^{2-}$ was added to the solution at the same time. After 1 week of incubation, the plants were harvested, washed with purified water, separated into roots and shoots, and subsequently freeze-dried, while a subsample of fresh root was treated immediately for TEM-EDX analysis.

2.2. Analysis of Hg and K in the plant samples

Freeze-dried plant materials were homogenized using an agate mortar and pestle. Total Hg content was determined in solid

samples via thermal decomposition to Hg^0 using a Lumex RA-915 + Hg analyzer equipped with a PYRO-915 + pyrolysis attachment (Lumex Co., Russia), which has a detection limit of 0.5–2 ng g^{-1} (Sholupov et al., 2004). To measure K, approximately 0.1 g of plant sample was weighed separately into 15 mL Teflon tubes and digested in an electric blast drying oven at 160 °C for 15 h using a mixture of sub-boiling distilled HNO_3 and HF (15:1, v/v). The digested solution was heated until the acid was reduced to a volume of 0.5–1 mL, which was reconstituted to 10 mL with 2% HNO_3. The K concentrations in solution were determined using inductively coupled plasma-optical emission spectrometry (Vista-MPX, Varian Inc.).

2.3. μ-XRF analysis

Plants collected from the Hg20 and Hg20 + thiosulphate treatments were analyzed using μ-XRF. The method for making plant cross sections was modified from Zhang et al. (2011). Fresh root (0.5 cm) and stem (0.5 cm) subsamples were frozen and fixed immediately on specimen disks using deionized water in an actively cooled quick freezing shelf (−30 °C). Cross-sections (60 μm thick) of root and stem samples were cut with a cryostat (CM3050 S, Leica), laid onto XRF film (Well Group Scientific, USA), and freeze-dried at −50 °C for 48 h. Micro X-ray fluorescence spectroscopy was performed on two stem (one-quarter) and two root (one-half) cross-sections of both control and thiosulphate treatments and measured at the beamline BL15U1 of the Shanghai Synchrotron Radiation Facility (SSRF), Shanghai, China. The electron energy and maximum ring current of the SSRF storage ring were 3.5 GeV and 300 mA, respectively. Fluorescence maps of Hg and K were obtained by scanning the samples under a monochromatic beam with a step size of 15 × 15 μm^2 and a dwell time of 1 s per step. A Si (Li) detector (PGT Inc. LS 30143-DS) was used to collect the XRF signals (Zhang et al., 2015b).

2.4. Microscope optical images

Fresh Hg20 subsamples were fixed in 2.5% glutaraldehyde (pH 7.0) for 4 h and rinsed with 0.1 M phosphate buffered saline (PBS) for 45 min. Samples were further fixed in 1% osmic acid made from 0.1 M PBS for 4 h and dehydrated with ethanol and acetone. Then, samples were embedded in Epon 812 epoxy resin. Stem and root cross-sections 1–2 μm thick were cut using a Leica ultramicrotome. The cross-sections were dyed with toluidine blue and optical images were obtained with a microscope.

2.5. TEM-EDX analysis

The pretreatment protocol of making root cross section for TEM-EDX analysis was the same as the microscope optical images. Serial ultrathin sections (72 nm) from the root were cut with a diamond knife, mounted on Cu grids, and then analyzed using an analytical transmission electron microscope (Tecnai G^2 F20 S-TWIN TMP, FEI Co., America) operated at 200 kV. The instrument is equipped with the hardware, which enable us to do the energy dispersive X-ray (EDX spectra), and selected area electron diffraction (SAED) pattern measurements. The EDX spectra and the SAED patterns could provide the information of the chemical compositions and the amorphous/crystalline nature of the selected particles, respectively.

2.6. Data analysis and quality control

The standard reference material GBW10020 (orange's foliage, Institute of Geophysical and Geochemical Exploration, China) was used for plant analytical quality control. The measured average total Hg and K concentrations of the reference material were 0.15 ± 0.01 mg kg^{-1} and 7.5 ± 0.3 mg g^{-1} ($n = 3$), which were comparable with the certified values of 0.15 ± 0.02 mg kg^{-1} and 7.7 ± 0.4 mg g^{-1}, respectively. The relative percentage difference of sample replicates by the plant was <7%. Color-coded composite images of Hg and K of root and stem cross-sections were mapped using Image-Pro Plus (ver. 6.0, Media Cybernetics, MA). Statistical analyses were conducted using SPSS for Windows (ver. 17.0, SPSS Inc, Illinois, USA). Results were considered significant at $p < 0.05$ and $p < 0.01$.

3. Results and discussion

3.1. Biomass yield and concentration of Hg and K in B. juncea

Addition of thiosulphate to the soils resulted in a significant decrease in the fresh weight except roots in Hg2.7 treatments, but did not affect significantly the dry weight of the harvested plant material except Hg20 treatments (Appendix A in Table S2), which might be explained by the loss of water and K from plants stressed by NH_4^+ and $S_2O_3^{2-}$ salts added to the soil through thiosulphate treatment.

We recorded a noticeable increase in the Hg concentrations in

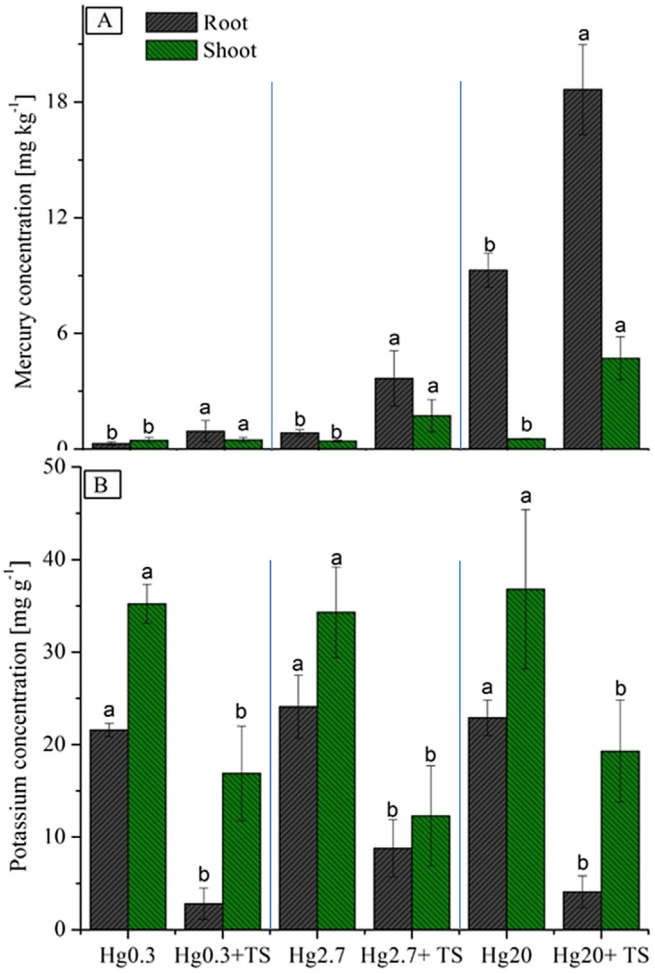

Fig. 1. Concentrations of mercury (A) and potassium (B) in the roots and shoots of the non-treated and thiosulphate-treated *B. juncea*; Bars denote standard deviation from the mean ($n = 3$). The different lower-case characters mean that the Hg or K concentration in the root or shoot was statistically different ($p < 0.05$) between the non-treated and thiosulphate-treated plants for each soil level of Hg. TS, thiosulphate.

the roots of the non-treated plants as a function of increasing Hg level in the soil (Fig. 1A). However, there was no obvious effect of soil Hg levels on Hg concentrations in the shoots of the non-treated plants (Fig. 1A). These results suggest limited translocation of Hg from roots to aboveground tissues in the non-treated plants, which is in agreement with Wang et al. (2011), who found that Hg was mainly concentrated in the root of *Chenopodium glaucum*, and its translocation of Hg from roots to shoots was of minor importance. The low concentrations of Hg in the shoots was also demonstrated by our μ-XRF results (section 3.2), which showed very low Hg intensity in the stem cross section.

Amendment of thiosulphate increased dramatically the concentration of Hg in the roots and shoots of *B.juncea* by 2–4.4 and 1–8.9 fold, respectively relative to the non-treated plants (Fig. 1A). For the thiosulphate-treated soil, the root and shoot Hg concentration increased as a function of Hg concentration in the soil, indicating that thiosulphate promotes the plant uptake of Hg from soils and the translocation of Hg from roots to shoots, which is comparable with previous studies (*e.g.* Moreno et al., 2005; Wang et al., 2011, 2012b; Lomonte et al., 2011) reporting the promotive effect of thiosulphate on Hg uptake by different plants.

Bioconcentration factor (BAF) refers to the plant tissue-to-soil Hg concentration ratio and is used to assess the capacity of the plants to accumulate Hg from soil. Transfer factor (TF) refers to the shoot-to-root Hg concentration ratio and is adopted to assess the capacity of plants to transport Hg from roots to aboveground tissues. Both BAF and TF are parameters which can be used to reflect the suitability of a plant species for phytoextraction purposes. The *B.juncea* grown in non-treated soils showed lower BAF_{root} and BAF_{shoot} compared to the plants grown in treated soils, indicating a limited ability of this species to accumulate Hg from soil without thiosulphate amendment (Appendix A in Table S3). Amendment of thiosulphate to soil resulted in a significant increase of 29%–786% and 100%–339% in BAF_{shoot} and BAF_{root} respectively, compared to the non-treated plants. The BAF value of our thiosulfate-treated *B. juncea* was higher than that of other plants reported by previous studies (Appendix A in Table S4). Our results demonstrate that thiosulphate treatment is effective in promoting the accumulation and translocation of Hg to the shoots of the *B.juncea*. Therefore, *B.juncea* in conjunction with thiosulphate can be effective in accumulating Hg from Hg-contaminated soil. However, this observation does not advance mechanistic understanding of how induced uptake happens.

The concentration of K in the root and shoot of non-treated plants was not affected by the Hg concentration of the soil ($p > 0.05$; Fig. 1B). However, the concentration of K was significantly lower ($p < 0.05$) in the roots and shoots of thiosulphate-treated plants relative to the non-treated plant of each level of soil Hg. It appears that amendment of thiosulphate to the soil might result in leakage of K from plant roots. The diminished K concentration in the plant shoots might be attributable to the limited translocation of K from roots to shoots as a result of the decreased K concentration in the roots.

3.2. Spatial distributions of Hg in B. juncea

Figs. 2 and 3 show the μ-XRF elemental maps and spatial distributions of both Hg and K in the scanned root and stem cross-sections of the non-treated and thiosulphate-treated plants and optical images obtained via microscopy. The intensity of element fluorescence is represented by different colors, and the purple-to-red color gradient corresponds to weaker and stronger intensities, respectively.

The μ-XRF elemental maps showed that the spatial distribution pattern of Hg in the root and stem of the treated plants differed from that of non-treated plants (Figs. 2 and 3). Mercury was mainly distributed in the roots than the stems of both the non-treated plants (Fig. 2-A,-C) and the thiosulphate-treated plants (Fig. 3-A, -C) as indicated by the higher intensity of Hg in the roots than in the stems. In the roots of both the non-treated and thiosulphate-treated plants, Hg was more distributed in the epidermis than the xylem. However, in the thiosulphate treated plants, the intensity of Hg in the xylem of roots was much stronger than in the xylem of non-treated plant roots. This means that thiosulphate promoted the transportation of Hg from the epidermis to the xylem of the roots, and thus enhanced its translocation from the roots to the stems as compared to the non-treated plants (Fig. 2-C *vs* Fig. 3-C). The critical step for the accumulation of elements such as Hg in aboveground tissues is their transportation from cortex to xylem where they can be loaded into the stem with water and inorganic nutrients as a function of transpiration (Oropeza-Garcia et al., 2014). Thus when Hg was loaded from the xylem of the root to the stem, it was mainly sequestered by the vascular bundles of the stem. These evidences indicate that application of thiosulphate to the soil may alter the pathway of transportation of Hg in the plant tissues. Such alteration largely enhances the uptake of Hg by the plant.

The greater distribution of Hg in the epidermis of the roots might be explained by the complexation of Hg with thiol-containing polypeptides of roots (Carrasco-Gil et al., 2013; Dago et al., 2014). Therefore, the majority of Hg would be accumulated by the roots, and potentially some of the metal loading could be transported to aboveground tissues (Iglesia-Turino et al., 2006). Thiosulphate-induced transportation of Hg from the epidermis to xylem may suggest a weaker effect of thiols on sequestering of Hg in the roots. This may be interpreted as uptake of Hg thiosulphate complexes by roots when thiosulphate was added to the soil and the limited binding of these complexes by the thiols in the epidermis of the root (Lomonte et al., 2014). A strong intensity of Hg was found in the vascular bundle of the stem tissues of treated plant (Fig. 3-C). The vascular bundle is the main conduction tissue for elements transported from roots to aboveground tissues, and contains two main types of conduction tissues, the xylem and phloem. Water and inorganic nutrients are transported mainly from roots to shoots by the xylem, while photosynthetic products such as carbohydrates are transported from leaf to root tissues via the phloem. We propose that Hg was transported from roots to shoots by the stem xylem.

3.3. Spatial distributions of K in the plants and its implications for Hg uptake

The μ-XRF elemental maps showed that the spatial distribution pattern of K was different from that of Hg (Fig. 2-C,-D and 3-C,-D). Potassium was mainly distributed in the stems over the roots of both the non-treated and thiosulphate-treated plants, as more clearly indicated by the higher intensity of K in the stem than in the root.

In the non-treated plants, K was mainly distributed across the epidermis and xylem of the root, while it was concentrated in the cortical cells and vascular of the stem. Application of thiosulphate altered the spatial distribution of K in both the root and stem. In the root, K was distributed throughout the whole cross-section, and the strongest intensity was observed in the epidermis; while, in the

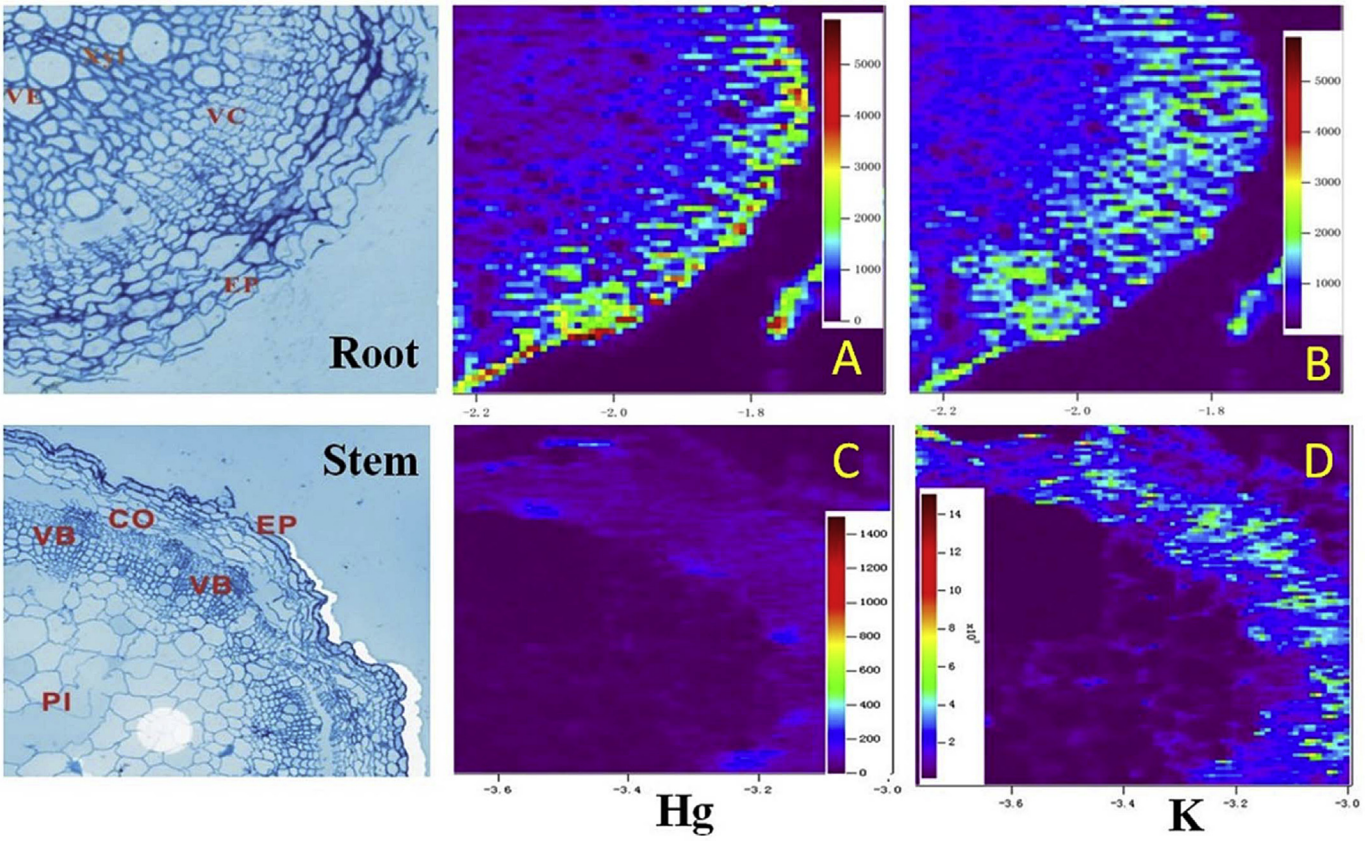

Fig. 2. Micro-X-ray fluorescence (μ-XRF) elemental maps for Hg and K of root and stem cross-sections of the non-treated plants. A: μ-XRF image of Hg of root cross section; B:μ-XRF image of K of root cross section; C: μ-XRF image of Hg of stem cross section; D: μ-XRF image of K of stem cross section. EP, epidermis; VC, vascular cambium; VE, vessels; Xyl, xylem.VB, vascular bundle; CO, cortex; PI, pith.

stem, K was mainly accumulated in the epidermis. This observation may result from the leakage of K from the cortex or xylem to the epidermis where some K remained in the epidermis at the time of harvest (Fig. 3-B, D). The higher intensity of K in the epidermis of thiosulphate-treated plants compared to the non-treated plants indicates that amendment of thiosulphate to the soil caused re-distribution of K in the plant tissues. The evidence presented here suggests that thiosulphate caused sufficient physiological damage to the plasma membrane of the root to effect leakage of K. The plasma membrane acts as the main barrier to exclude toxic elements from plant tissues. Most essential elements pass through this barrier via a mechanism mediated by the specific protein transporters embedded in the plasma membrane (Quick and Javitch, 2007); but protein transporters which mediate the passage of Hg across the plasma membrane are not yet clear. Elements can pass through the plasma membrane though damaged sites of the plasma membrane (Luo et al., 2006).

In our work, application of thiosulphate resulted in leakage of K from roots, which is an indication of damage of the plasma membrane. In general, the concentration of K in the cytosolic space is about two orders of magnitude greater than in the extracellular space due to the active uptake of K from environment by plants (Dreyer and Uozumi, 2011). The loss of electrochemical gradient can result in the leakage of K from the intracellular space to the extracellular space and this can be caused by physiological damage, triggered by physical/chemical/biological root stress (*e.g.* adding chemicals, salinity, heavy metals, hyperthermia) (Demidchik et al., 2014). Prior studies (*e.g.* Repka et al., 2013) reported that plants exposed to Hg^{2+} solution suffer depolarization of the root plasma membrane, and subsequently leakage of electrolyte. However, in our study, a similar concentration of K in the root of *B. juncea* for the non-contaminated soil (Hg 0.3 mg kg^{-1}) and the contaminated soils (Hg 2.7 and 20 mg kg^{-1}) indicates that any Hg-induced leakage is of minor importance. This phenomenon may be attributable to the relatively low toxicity of Hg because Hg^{2+} would be complexed with organic matter and converted to less bioavailable forms of Hg in soil such as nano particulate β-HgS (Manceau et al., 2015).

We propose that Hg-thiosulphate complexes enter plant roots through the plasma membrane damaged by thiosulphate (Fig. 3-A). We substantiate this with the observation that the decrease of K concentration in the root is associated with bioaccumulation of Hg as demonstrated by the significant negative correlation between Hg-BAF_{root} and the K concentration of the root of *B.juncea* (Appendix A in Fig. S1). Mercury can be efficiently loaded into the shoot as a function of thiosulphate treatment as shown by the 10-fold higher Hg concentration for this treatment relative to the non-treated control.

3.4. Subcellular distribution of Hg in the roots of B.juncea

The spatial image of Hg in the root of the thiosulphate treated plant showed that metal was transported from the epidermis to the xylem (Fig. 3-A). Specific transportation of Hg from the cortex to the xylem was observed, as this may have happened via the affected

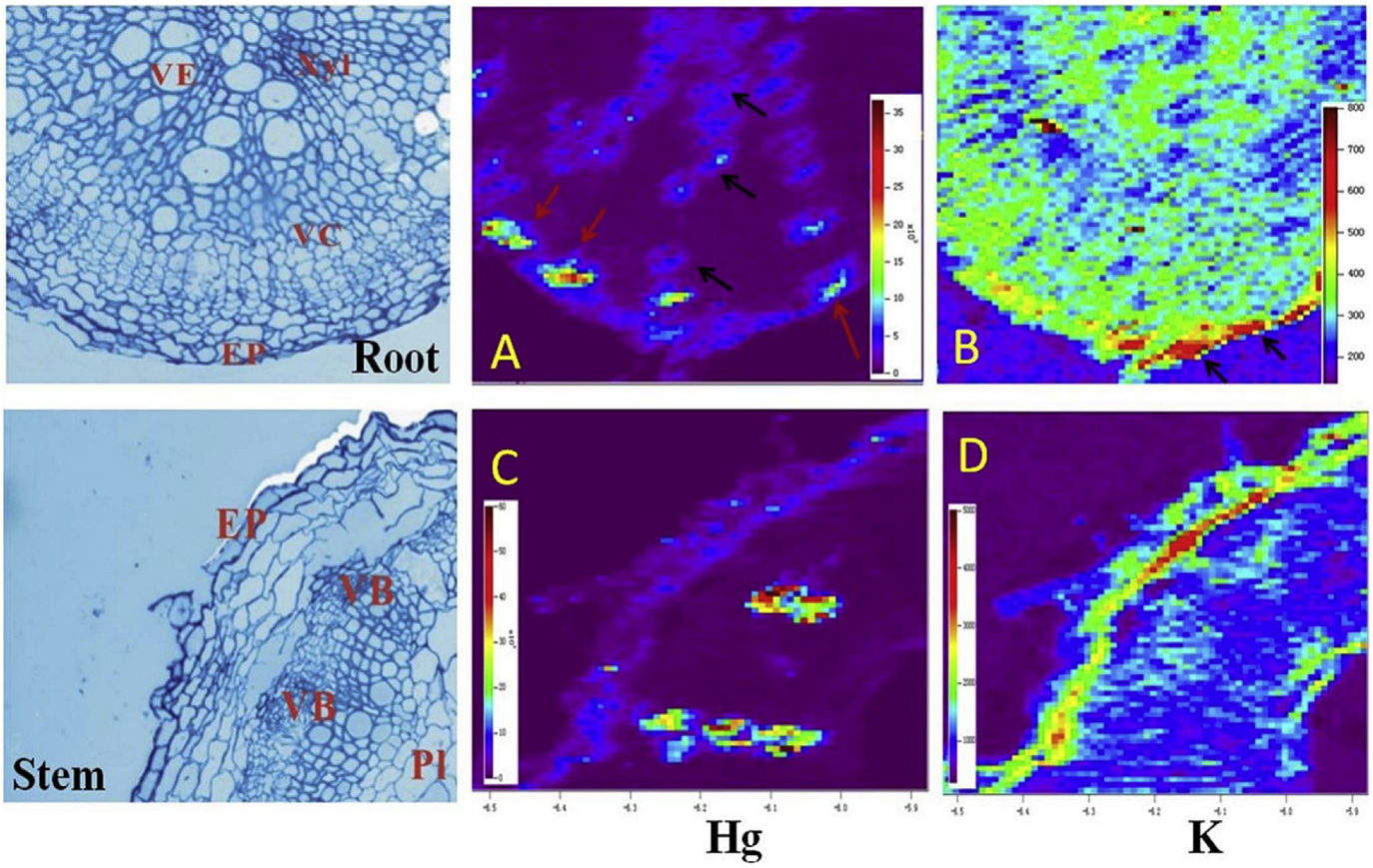

Fig. 3. Micro-X-ray fluorescence (μ-XRF) elemental maps for Hg and K of root and stem cross-sections of thiosulphate-treated plants. A: μ-XRF image of Hg of root cross section; B: μ-XRF image of K of root cross section; C: μ-XRF image of Hg of stem cross section; D: μ-XRF image of K of stem cross section. E.P, epidermis; VC, vascular cambium; VE, vessels; Xyl, xylem; VB, vascular bundle; PI, pith. The black arrows on Fig A point to the parenchyma cells of the xylem where Hg were transported; The red arrows on Fig A point to the site of Hg "hotpot" where the plasma membrane might be damaged by thiosulphate; The black arrows on Fig B point to the site of epidermis where K might be leached. (For interpretation of the references to color in this figure legend, the reader is referred to the Web version of this article.)

parenchyma cells (Fig. 3-A) by thiosulphate and became permeable to Hg complexes. Ciamporova (1993) reported that parenchyma cell in the cortex of roots are typically composed of living cells that are unspecialized in structure, thin-walled, and therefore sensitive to chemical stress. Therefore, to further verify whether the Hg was localized at the parenchyma cell, plant was incubated with Hg^{2+} and $S_2O_3^{2-}$ under hydroponic condition, and its root (Hg concentration = 486 mg kg^{-1}) was analyzed using TEM-EDX spectroscopy.

We observed a number of electron-dense black deposits with a scale of up to 30 nm surrounding the root cell wall of the thiosulphate-treated plants (Fig. 4,-A, -B,-C). Energy Dispersive X-ray spectroscopy analysis showed the presence of both Hg and S in these deposits with an approximate molar Hg:S ratio of 1:1, which indicates that Hg was mainly associated with S during transportation in the root. These observations agree with those of Wang et al. (2012b), who used X-ray absorption near edge structure (XANES) spectroscopy to study the speciation of Hg in thiosulphate-treated plants and found that the dominant speciation of Hg in the root was in forms similar to HgS complexes. In the current study we used selected area electron diffraction (SAED) analysis to further characterize the observed nano clusters; no crystallization was observed (Fig. 4,-D, -E, -F). Therefore, Hg was present as amorphous nano Hg-S clusters in the thiosulphate treated plants. Besides the electron-dense black deposits distributed in the cell wall, several similar deposits were observed within parenchyma cells (Fig. 4-A). However, no Hg signals were detected using EDX spectroscopy (Figure not shown). We propose that Hg was transported through the pathway of the extracellular space of the root (*e.g.* apoplast pathway).

Using the mechanistic information gained from the current work, we propose a model for plant uptake of solubilized Hg (Appendix A in Fig. S2). Damage to the plasma membrane causes the leakage of K from the tissues of roots, and Hg enters the roots via the affected plasma membrane. The Hg-S complexes are then further loaded to the shoot via the vascular bundles.

4. Conclusions

Thiosulphate promoted the accumulation of Hg, but reduced the accumulation of K, by *B.juncea*. The negative correlation between root Hg-BAF and the root K concentration indicated that the accumulation of Hg by roots was associated with leakage of K. This leakage was further demonstrated by μ-XRF results showing that K was moved to the epidermis after thiosulphate treatment. Mercury was sequestered mainly in the epidermis of the non-treated roots, while Hg was transferred to the xylems of roots and the vascular bundles of stems, when thiosulphate was added to the soils. This movement was associated with sulfur as detected by TEM-EDX spectroscopy. This mechanistic knowledge provides new insight into how thiosulphate-induced Hg is taken up by plants, and is important for improving Hg phytoextraction efficacy using bioenergy crops such as *B.juncea* via application of thiosulphate. Futher studies should verify our results under field conditions.

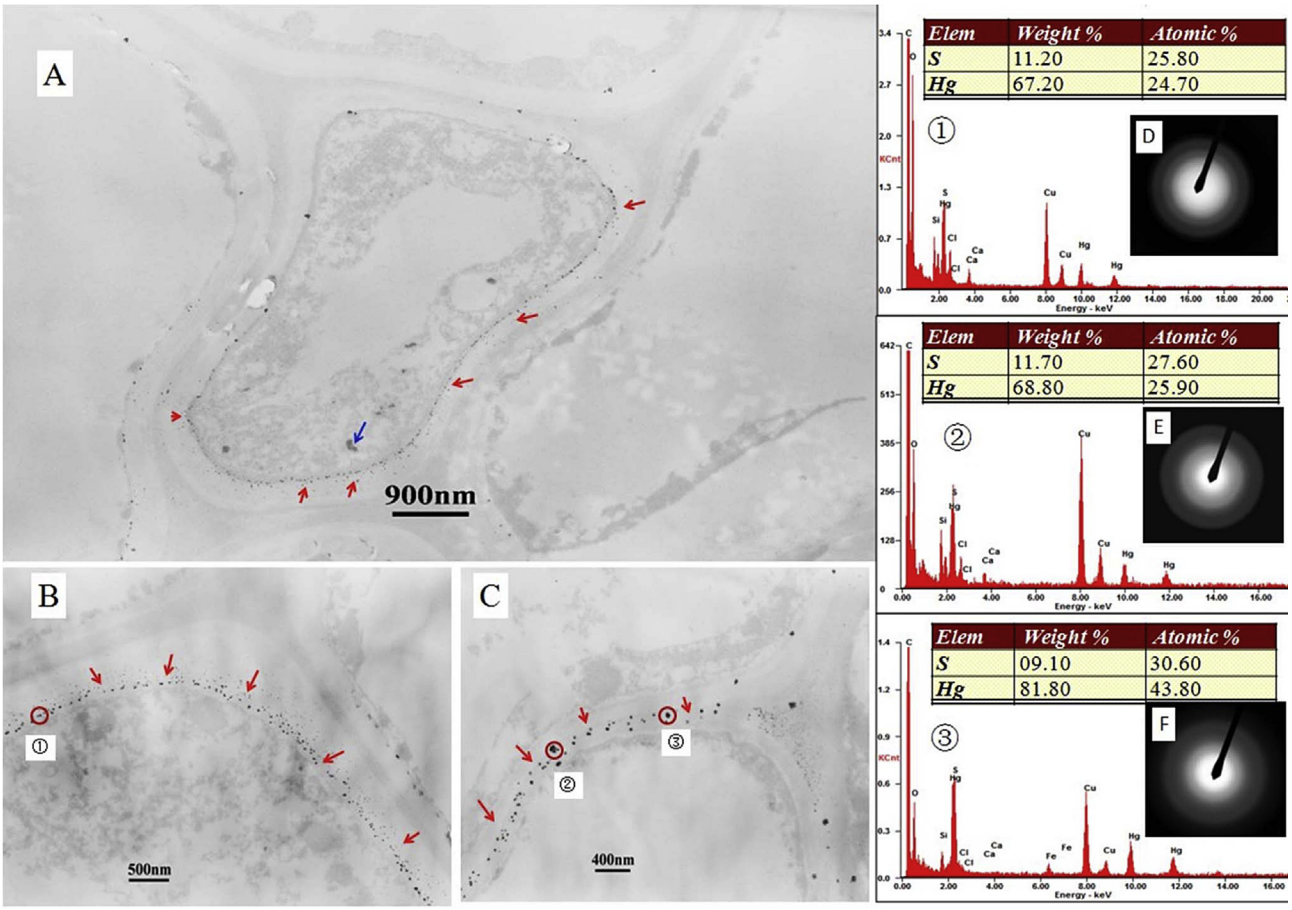

Fig. 4. Transmission Electron Microscopy (TEM) images and Energy Dispersive X-ray (EDX) spectra of the root cross sections of the thiosulphate treated plant. The intensity of copper resulted from the copper grid holder. The red arrows point to the black nano-cluster surrounding the cell of root; the blue arrows point to the black deposits where no Hg signals were detected. The numbers (①,②,③) on the figure B and C means the sites which were subjected to both EDX and SAED spectroscopy analysis. (For interpretation of the references to color in this figure legend, the reader is referred to the Web version of this article.)

Acknowledgements

This study was financed by the Natural Science Foundation of China (41573082, 41703116, 41303068), the Science and Technology Foundation of Guizhou Province (Nos. [2013]2218 and [2014] 2169), the Youth Innovation Promotion Association of the Chinese Academy of Sciences, and the Opening Fund of the State Key Laboratory of Environmental Geochemistry (SKLEG2017907, SKLEG2017912).We thank the German Alexander von Humboldt Foundation for the financial support of the postdoctoral fellowship of Dr.Jianxu Wang (Ref 3.5—1186537-CHN-HFST-P) and the experienced researcher's fellowship of Prof. Dr. Sabry M. Shaheen (Ref 3.4 - EGY - 1185373 - GF-E) at the University of Wuppertal, Germany. Many thanks go to the BL15U1 beamstation at Shanghai Synchrotron Radiation Facility for supporting the μ-XRF analysis.

Appendix A. Supplementary data

Supplementary data related to this article can be found at https://doi.org/10.1016/j.envpol.2018.07.065.

References

Antoniadis, V., Shaheen, S.M., Boersch, J., Frohne, T., Du Laing, G., Rinklebe, J., 2017a. Bioavailability and risk assessment of potentially toxic elements in garden edible vegetables and soils around a highly contaminated former mining area in Germany. J. Environ. Manag. 186, 192–200.

Antoniadis, V., Levizou, E., Shaheen, S.M., Ok, Y.S., Sebastian, A., Baum, C., Prasad, M.N.V., Wenzel, W.W., Rinklebe, J., 2017b. Trace elements in the soil-plant interface: Phytoavailability, translocation, and phytoremediation–A review. Earth Sci. Rev. 171, 621–645.

Beata, S., Katarzyna, K., 2012. Leaching of mercury during phytoextraction assisted by EDTA, KI and citric acid. J. Chem. Technol. Biotechnol. 87, 1360–1365.

Beckers, F., Rinklebe, J., 2017. Cycling of mercury in the environment: sources, fate, and human health implications-a review. Crit. Rev. Environ. Sci. Technol. 47, 693–794.

Carrasco-Gil, S., Siebner, H., LeDuc, D.L., Webb, S.M., Millan, R., Andrews, J.C., Hernandez, L.E., 2013. Hg localization and speciation in plants grown hydroponically or in a natural environment. Environ. Sci. Technol. 47, 3082–3090.

Ciamporova, M., 1993. Transfer cells in the vascular parenchyma of roots. Biol. Plantarum 35, 261–266.

Dago, A., Gonzalez, I., Arino, C., Martinez-Coronado, A., Higueras, P., Diaz-Cruz, J.M., Esteban, M., 2014. Evaluation of Hg stress in plants from the almaden mining district by analysis of phytochelatins and their Hg complexes. Environ. Sci. Technol. 48, 6256–6263.

Demidchik, V., Straltsova, D., Medvedev, S.S., Pozhvanov, G.A., Sokolik, A., Yurin, V., 2014. Stress-induced electrolyte leakage: the role of K-permeable channels and involvement in programmed cell death and metabolic adjustment. J. Exp. Bot 65, 1259–1270.

Dreyer, I., Uozumi, N., 2011. Potassium channels in plant cells. FEBS J. 278, 4293–4303.

Feng, X., Qiu, G., 2008. Mercury pollution in Guizhou, southwestern China-An overview. Sci. Total Environ. 400, 227–237.

Iglesia-Turino, S., Febrero, A., Jauregui, O., Caldelas, C., Araus, J.L., Bort, J., 2006. Detection and quantification of unbound phytochelatin2 in plant extracts of Brassica napus grown with different levels of Hg. Plant Physiol. 142, 742–749.

Lomonte, C., Doronila, A., Gregory, D., Baker, A.J.M., Kolev, S.D., 2011. Chelate-assisted phytoextraction of Hg in biosolids. Sci. Total Environ. 409, 2685–2692.

Lomonte, C., Wang, Y.D., Doronila, A., Gregory, D., Baker, A.J.M., Siegele, R., Kolev, S.D., 2014. Study of the spatial distribution of Hg in roots of vetiver grass (*chrysopogon zizanioides*) by micro-pixe spectrometry. Int. J. Phytoremediation

16, 1170–1182.
Luo, C.L., Shen, Z.G., Li, X.D., Baker, A.J.M., 2006. The role of root damage in the chelate-enhanced accumulation of lead by Indian mustard plants. Int. J. Phytoremediation 8, 323–337.
Luo, C.L., Shen, Z.G., Li, X.D., 2008. Hot NTA application enhanced metal phytoextraction from contaminated soil. Water, Air, Soil Pollut. 188, 127–137.
Manceau, A., Lemouchi, C., Enescu, M., Gaillot, A.C., Lanson, M., Magnin, V., Glatzel, P., Poulin, B.A., Ryan, J.N., Aiken, G.R., Gautier-Luneau, I., Nagy, K.L., 2015. formation of mercury sulfide from Hg(II)-Thiolate complexes in natural organic matter. Environ. Sci. Technol. 49, 9787–9796.
Moreno, F.N., Anderson, C.W.N., Stewart, R.B., Robinson, B.H., Ghomshei, M., Meech, J.A., 2005. Induced plant uptake and transport of Hg in the presence of sulphur-containing ligands and humic acid. New Phytol. 166, 445–454.
Oropeza-Garcia, N., Hausler, R., Glaus, M., 2014. Transport of heavy metals in materials with diameter analogous to xylem vessels. Int. J. Environ. Res. 8, 123–132.
Pedron, F., Petruzzelli, G., Barbafieri, M., Tassi, E., 2013. Remediation of a Hg-Contaminated industrial soil using bioavailable contaminant stripping. Pedosphere 23, 104–110.
Quick, M., Javitch, J.A., 2007. Monitoring the function of membrane transport proteins in detergent-solubilized form. Proc. Natl. Acad. Sci. Unit. States Am. 104, 3603–3608.
Repka, V., Fiala, R., Čarná, M., Pavlovkin, J., 2013. Membrane potential differences and viability of grapevine root cells treated with $HgCl_2$. Plant Soil Environ. 59, 353–358.
Rodríguez, L., Alonso-Azcárate, J., Villaseñor, J., Rodríguez-Castellanos, L., 2016. EDTA and hydrochloric acid effects on mercury accumulation by Lupinus albus. Environ. Sci. Pollut. Res. 23, 24739–24748.
Shaheen, S.M., Rinklebe, J., 2015a. Phytoextraction of potentially toxic elements by Indian mustard, rapeseed, and sunflower from a contaminated riparian soil. Environ. Geochem. Health 37, 953–967.
Shaheen, S.M., Rinklebe, J., 2015b. Impact of emerging and low cost alternative amendments on the (im)mobilization and phytoavailability of Cd and Pb in a contaminated floodplain soil. Ecol. Eng. 74, 319–326.
Shiyab, S., Chen, J., Han, F.X., Monts, D.L., Matta, F.B., Gu, M., Su, Y., Masad, M.A., 2009. Mercury-induced oxidative stress in Indian mustard (*Brassica juncea L.*). Environ. Toxicol. 24, 462–471.
Sholupov, S., Pogarev, S., Ryzhov, V., Mashyanov, N., Stroganov, A., 2004. Zeeman atomic absorption spectrometer RA-915+for direct determination of mercury in air and complex matrix samples. Fuel Process. Technol. 85, 473–485.
Wang, J.X., Feng, X.B., Anderson, C.W.N., Qiu, G.L., Ping, L., Bao, Z.D., 2011. Ammonium thiosulphate enhanced phytoextraction from Hg contaminated soil-Results from a greenhouse study. J. Hazard Mater. 186, 119–127.
Wang, J.X., Feng, X.B., Anderson, C.W.N., Xing, Y., Shang, L.H., 2012a. Remediation of mercury contaminated sites-A review. J. Hazard Mater. 221, 1–18.
Wang, J.X., Feng, X.B., Anderson, C.W.N., Wang, H., Zheng, L.R., Hu, T.D., 2012b. Implications of Hg speciation in thiosulphate treated plants. Environ. Sci. Technol. 46, 5361–5368.
Wang, J.X., Feng, X.B., Anderson, C.W.N., Wang, H., Wang, L.L., 2014. Thiosulphate-induced Hg accumulation by plants: metal uptake and transformation of Hg fractionation in soil- results from a field study. Plant Soil 375, 21–33.
Wang, J.X., Xia, J.C., Feng, X.B., 2017. Screening of chelating ligands to enhance Hg accumulation from historically Hg-contaminated soils for phytoextraction. J. Environ. Manag. 186, 233–239.
Wang, S.Q., Zhong, T.Y., Chen, D.M., 2016. Spatial distribution of mercury (Hg) concentration in agricultural soil and its risk assessment on food safety in China. Sustainability 8, 1–12.
Wei, M.K., Wu, Q.P., Huang, Q., Wu, J.L., Zhang, J.M., 2008. Plasma membrane damage to Candida albicans caused by chlorine dioxide (ClO_2). Lett Appl Microbiol. 47, 67–73.
Zhang, H., Feng, X.B., Larssen, T., Qiu, G.L., Vogt, R.D., 2010. In inland China, rice, rather than fish, is the major pathway for MethylHg exposure. Environ. Health Perspect. 118, 1183–1188.
Zhang, J., Tian, S.K., Lu, L.L., Shohag, M.J.I., Liao, H.B., Yang, X.E., 2011. Lead tolerance and cellular distribution in *Elsholtzia splendens* using synchrotron radiation micro-X-ray fluorescence. J. Hazard Mater. 197, 264–271.
Zhang, L., Wang, S.X., Wang, L., Wu, Y., Duan, L., Wu, Q.R., Wang, F.Y., Yang, M., Yang, H., Hao, J.M., Liu, X., 2015a. Updated emission inventories for speciated atmospheric Hg from anthropogenic sources in China. Environ. Sci. Technol. 49, 3185–3194.
Zhang, L.L., Yan, S., Jiang, S., Yang, K., Wang, H., He, S.M., Liang, D.X., Zhang, L., He, Y., Lan, X.Y., 2015b. Hard X-ray micro-focusing beamline at SSRF. Nucl. Sci. Tech. 26, 060101.
Zhao, F.J., Ma, Y.B., Zhu, Y.G., Tang, Z., McGrath, S.P., 2015. Soil contamination in China: current status and mitigation strategies. Environ. Sci. Technol. 49, 750–759.
Zheng, Y.H., Jia, A.J., Ning, T.Y., Xu, J.L., Li, Z.J., Jiang, G.M., 2008. Potassium nitrate application alleviates sodium chloride stress in winter wheat cultivars differing in salt tolerance. J. Plant Physiol. 165, 1455–1465.
Zhou, J., Liu, H., Du, B., Shang, L., Yang, J., Wang, Y., 2015. Influence of soil mercury concentration and fraction on bioaccumulation process of inorganic mercury and methylmercury in rice (*Oryza sativa L.*). Environ. Sci. Pollut. Res. 22, 6144–6154.